CHEMICAL & PHARMACEUTICAL BULLETIN

Vol. 36, No. 9 September 1988

Regular Articles

[Chem. Pharm. Bull. 36(9)3239—3247(1988)]

Study on Conformations–Biological Activities Relationships for Podophyllotoxin Analogues Based on Crystal Structure of Deoxypodophyllotoxin (Anthricin)

DAISUKE YAMAMOTO,* HIROFUMI OHISHI, MITSUGI KOZAWA, YOSHIHIKO INAMORI, TOSHIMASA ISHIDA and MASATOSHI INOUE

Osaka University of Pharmaceutical Sciences, 2–10–65 Kawai, Matsubara, Osaka 580, Japan

(Received February 8, 1988)

The conformation of deoxypodophyllotoxin (anthricin) was determined by X-ray crystal structure analysis. Based on this data, possible conformations of seven other podophyllotoxin analogues were optimized using molecular mechanics calculation, and their atomic charges and molecular dipole moments were then calculated using CNDO/2 method. The relationships between these parameters and their biological activities were examined by simple regression analyses. It was suggested that the deoxyribonucleic acid (DNA) strand breakage activity is significantly dependent on the distribution of the atomic charges in the podophyllotoxin structure, and the antimicrotubule activity on the steric parameters.

Keywords——podophyllotoxin analogue; deoxypodophyllotoxin; X-ray crystallography; molecular mechanics; atomic charge; dipole moment; conformational parameter; structure–activity relationship

Podophyllotoxin analogues shown in Fig. 1 have already been reported to show the different biological responses for the antimicrotubule[1-4] and deoxyribonucleic acid (DNA) strand breakage[1,5] activities, which are intimately related to cytotoxic and antitumor

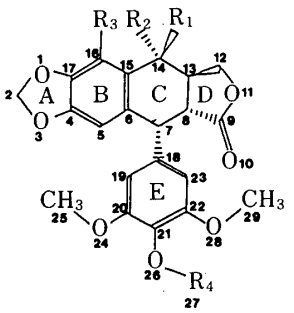

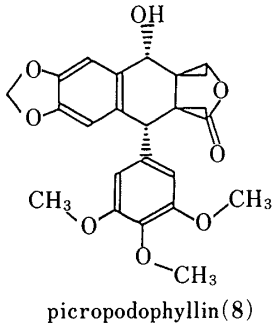

picropodophyllin(8)

podophyllotoxin analogues	R_1	R_2	R_3	R_4
4-deoxypodophyllotoxin (**1**)	H	H	H	CH_3
podophyllotoxin (**2**)	H	OH	H	CH_3
epipodophyllotoxin (**3**)	OH	H	H	CH_3
4′-demethylpodophyllotoxin (**4**)	H	OH	H	H
4′-demethylepipodophyllotoxin (**5**)	OH	H	H	H
α-peltatin (**6**)	H	H	OH	H
β-peltatin (**7**)	H	H	OH	CH_3

Fig. 1. Chemical Structures of Podophylotoxin Analogues and Atomic Numbering of **1**

activities respectively. The relationships between these activities and chemical structures have been proposed by Long *et al.*[1]; the configuration of the hydroxyl group at C-ring is highly related to both two activities. The hydroxyl group at R_4 site of E-ring is absolutely necessary for DNA single strand breakage (SSB) activity, while this group has no significant effect for the antimicrotubule activity. This latter activity is largely dependent on the conformation of the C–D ring junction.

In this paper, for the purpose of a quantitative discussion of the relationship between the podophyllotoxin analogues and their biological activities, we deal with the X-ray crystal analysis of deoxypodophyllotoxin (**1**), the conformational predictions of the podophyllotoxin analogues (shown in Fig. 1) based on the crystal data of **1**, and the relationships of their steric and electrostatic parameters with the antimicrotubule and DNA SSB activities.

Deoxypodophyllotoxin (**1**) ($C_{22}H_{22}O_7$), called anthricin, was selected for X-ray analysis, because it has the basic structure of the analogue molecules and has been reported showing the antitumor, phytogrowth inhibition, and insecticidal activities.[6-9]

Results and Discussion

X-Ray Crystal Structure Analysis

The crystallographic data of **1** are as follows; $C_{22}H_{22}O_7$, $M_r = 398.4$, orthorhombic, space group $P2_12_12_1$, $a = 10.055(3)$, $b = 12.926(3)$, $c = 29.774(7)$ Å; volume $= 3870(2)$ Å^3, $Z = 8$, $D_c = 1.368$, $D_m = 1.362(1)$ g·cm^{-3}; μ(Cu$K\alpha$) $= 8.10$ cm^{-1}, and $F(000) = 1680$. The atomic numbering used for **1** and the other podophyllotoxin analogues in this study is shown in Fig. 1. As shown in Fig. 2, two crystallographically independent molecules in an asymmetric unit, named forms A and B, show very similar conformations to each other; some intramolecular torsion angles are given in Table I. A major conformational difference between forms A and B is found at the R_4 site of E-ring; the torsion angles of C20–C21–O26–C27 are $-103.1°$ for form A and $86.0°$ for form B. A minor one is also found in the orientation of E-ring with respect to C-ring and in the puckering of A-ring. In these conformations of **1**, however, the C–D ring junctions are both *trans*, A-rings are coplanar with B-rings, and E-rings are pseudo-axially attached to C-rings. These conformational characteristics, except for the orientation of E-ring with respect to C-ring and for the conformation of methoxy groups attached to E-ring, are commonly

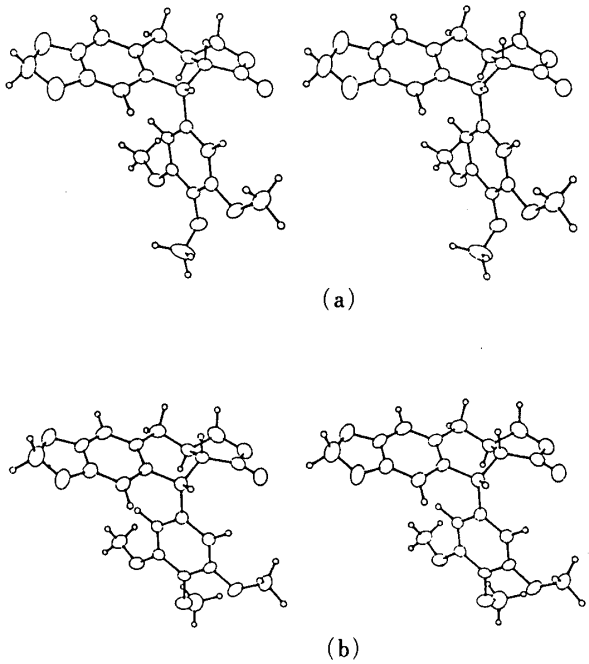

Fig. 2. Stereoscopic Drawings of the Two Crystallographically Independent Molecules of **1**

(a), form A; (b), form B.

TABLE I. Selected Torsion Angles of **1** Observed in Forms A and B with Estimated Standard Deviations in Parentheses

Bond	Angle (°)	
	Form A	Form B
C–D ring junction		
C15–C6–C7–C8	13.4 (6)	22.7 (5)
C6–C15–C14–C13	16.6 (6)	11.5 (7)
C6–C7–C8–C9	−170.7 (6)	−179.6 (4)
C15–C14–C13–C12	−163.8 (7)	−158.2 (6)
Orientation of E-ring with respect to C-ring		
C6–C7–C18–C19	42.4 (6)	21.8 (4)
C6–C7–C18–C23	−136.2 (5)	−158.5 (5)
C8–C7–C18–C19	−81.7 (7)	−100.4 (6)
C8–C7–C18–C23	99.7 (6)	79.3 (4)
Conformation of R_4 methoxy group		
C20–C21–O26–C27	−103.1 (6)	86.0 (7)
C22–C21–O26–C27	78.6 (6)	−94.3 (8)
Puckering of A-ring		
C17–O1–C2–O3	1.0 (7)	−8.9 (5)
C2–O1–C17–C4	−2.1 (6)	6.0 (7)
O1–C2–O3–C4	0.4 (7)	8.6 (6)
C2–O3–C4–C17	−1.8 (6)	−5.0 (6)
O3–C4–C17–O1	2.4 (5)	−0.9 (6)

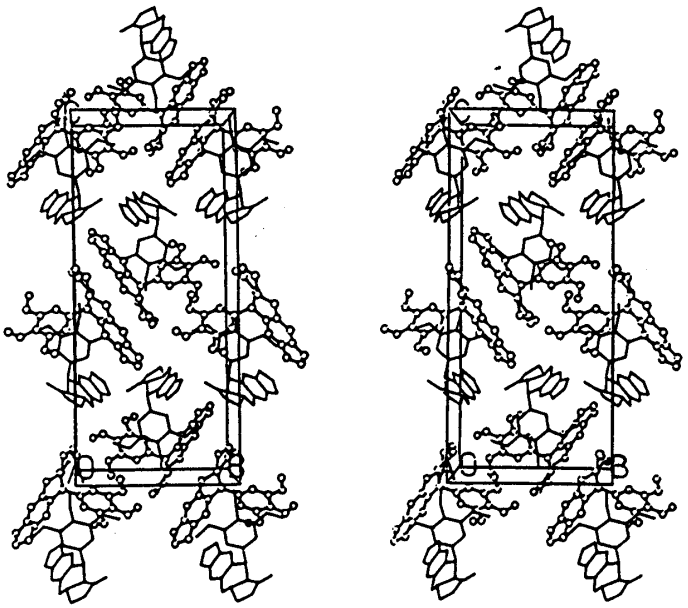

Fig. 3. Stereoscopic Drawings of the Molecular Packing of **1** Viewed along the *a*-Axis

Form A is represented by stick model and form B by ball-and-stick model.

found in the structures of other podophyllotoxin derivatives determined by X-ray crystallography.[10-12] The molecular packing viewed down the *a*-axis is shown in Fig. 3. The crystal structure is mainly stabilized by the Van der Waals contacts between the neighboring molecules; no hydrogen bond is found in this crystal. Both molecules of forms A and B are stabilized by significant ring stacking interactions (see Fig. 4). The average interplanar spacing and the dihedral angle between the A-rings of the forms A and B are 3.2 Å and 8.6 °, and those between the E-rings are 3.6 Å and 23.2 °, respectively.

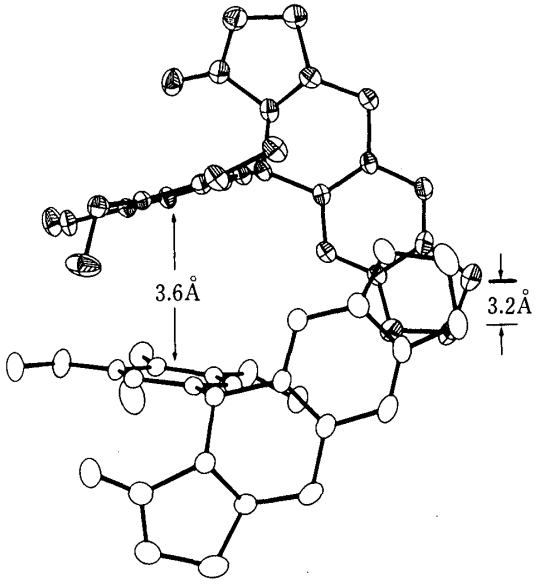

Fig. 4. Ring Stacking Interaction between Forms A and B

The average interplanar spacing of A-rings between forms A and B is 3.2 Å, and that of E-rings is 3.6 Å. Form B is expressed with open ellipses.

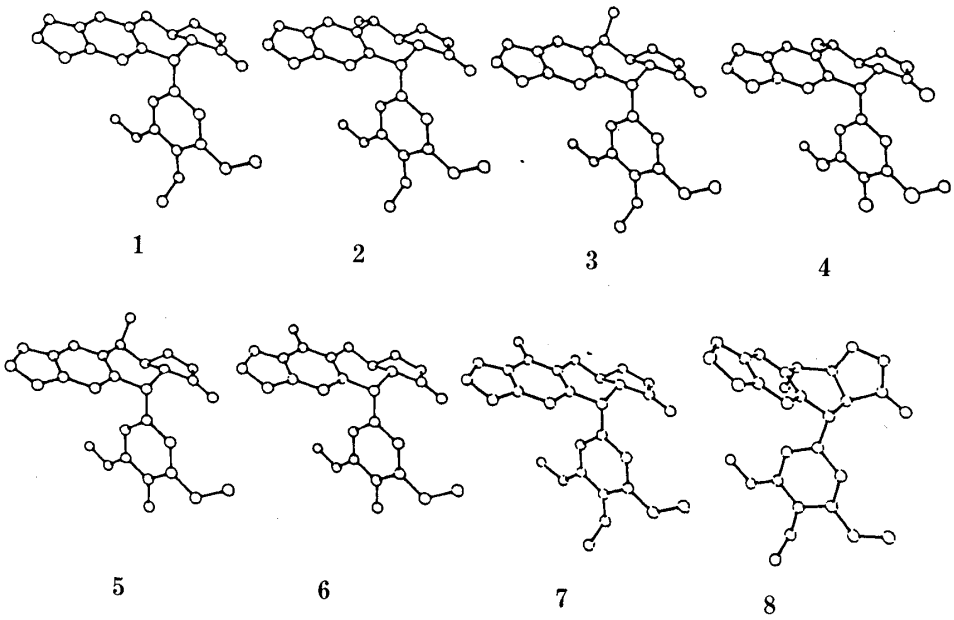

Fig. 5. Optimized Conformations of Podophyllotoxin Analogues

Relationships between Conformational Parameters and Biological Activities

Based on the atomic parameters of **1** obtained by the crystal analysis, possible conformations of seven analogues (**2**—**8**) were built (see Fig. 1). For picropodophyllin (**8**), which differs from **1** in the C–D ring junction, the probable conformation was estimated from the coupling constants of the proton nuclear magnetic resonance (^{1}H-NMR) spectra of deoxypicropodophyllin.[13] These possible conformations (**1**—**8**) were then applied to free-valence geometry optimization using force-field method.[14,15] The optimized conformations are shown in Fig. 5.

Coordinate shift values (X, Y and Z in Å) of each atom from the best plane of B-ring and from two planes perpendicular to this plane, were calculated respectively; the definitions of X, Y and Z directions are shown in Fig. 6. The atomic charge for each atom and the molecular dipole moments were calculated by CNDO/2 method.[16] The dipole moments and their components along X, Y and Z directions are listed in Table II. It is of interest to note that X-

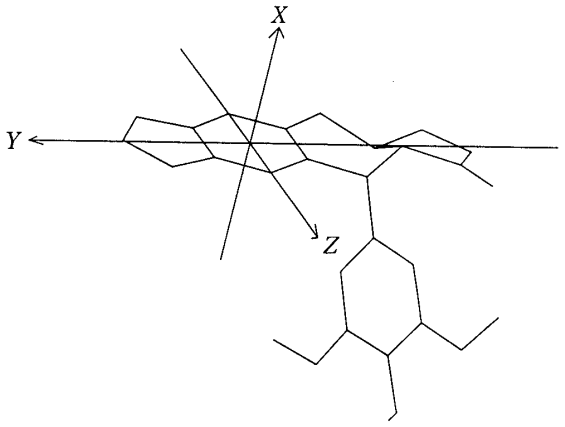

Fig. 6. Definition of Coordinate Shift Values

TABLE II. Three Components and Total Values of Dipole Moments Calculated by CNDO/2 Method

Analogue	Dipole moment (debye)			
	X	*Y*	*Z*	Total
1	3.66	4.06	−4.31	6.97
2	4.96	5.18	−4.06	8.24
3	2.67	5.85	−4.36	7.77
4	5.48	2.68	−3.51	7.04
5	3.20	3.38	−3.84	6.03
6	4.01	3.21	−3.18	6.04
7	3.50	5.71	−3.69	7.65
8	2.67	3.11	−4.70	6.24

TABLE III. Biological Activities of Podophyllotoxin Analogues

Analogue	Antimicrotubule[a)]	DNA SSB[b)]
1	4 (0.5)	2 (10^{-5})
2	4 (0.6)	1 (10^{-4})
3	2 (5.0)	1 (10^{-4})
4	4 (0.5)	3 (10^{-6})
5	3 (2.0)	4 (10^{-7})
6	4 (0.5)	2 (10^{-5})
7	4 (0.7)	1 (10^{-4})
8	1 (30)	1 (10^{-4})

a) Antimicrotubule activities were ranked as inhibition of microtubule assembly (ID_{50}) taken from ref. 1; the concentrations (μM) of drugs necessary to inhibit chicken brain microtubule assembly by 50% during a 30-min incubation period at 37 °C are shown in parentheses. *b*) DNA SSB activities were ranked as break frequencies taken from ref. 1; the concentrations (M) of drugs necessary to cause over 0.5 breaks per 10^8 nucleotides, when A549 cells were exposed to drugs for 1 h, are shown in parentheses.

and *Y*-components of the dipole moments are largely dependent on the positions of O10, O11 and O14 (hydroxyl oxygens attached to C14 or C16), and the *Y*- and *Z*-components are significantly affected by the negative atomic charge of O26; the CNDO/2 calculation shows that the demethylation at R_4 site increases the highest occupied molecular orbital (HOMO) coefficient of O26 atom significantly, and consequently this change increases nucleophillic specificity of O26 atom.

The relationships between these conformational parameters and biological activities were next considered; two activities (antimicrotubule and DNA SSB activities) of these analogues are listed in Table III. We applied the linear regression analyses on the following three groups; (1) all eight analogues, (2) seven analogues except for **8**, and (3) five analogues except for **6**, **7** and **8**. For each group, respective correlation coefficients were calculated for all pairs between the activities and the conformational parameters of shift values, atomic charges and dipole moments. The pairs with high correlation coefficients are summarized in Table IV, along with the results of *t*-tests.[17] Large negative correlation coefficients between the antimicrotubule activity and the shift values of O14 and between the DNA SSB activity and the atomic charge of O26 are observed for all groups. This result means that these biological activities are more importantly related with the hydroxyl O14 and methoxy O26 atoms respectively. In the groups (1) and (3), high correlation coefficients between the *X*-component of the dipole

TABLE IV. Pairs Showing High Correlation Coefficients (R) between Conformational Parameters (X) and Activities (Y) from Linear Regression Analyses ($Y=aX+b$)

Activity	Conformational parameters	R	a	b
Group 1 ($n=8$)				
Antimicrotubule	Shift-X on O11	$-0.77^{a)}$	−0.86	3.45
	Shift-X on C23	$0.82^{a)}$	11.91	18.19
	Shift-Z on O11	$-0.77^{a)}$	−5.18	3.59
	Shift-Z on C23	$-0.79^{a)}$	10.26	32.98
	Shift-Z on O14[c)]	$-0.95^{b)}$	−2.39	−2.39
	Dipole-X	$0.73^{a)}$	0.84	0.09
	Dipole-Z	0.72	1.67	9.86
DNA SSBs	Charge on O26	$-0.82^{a)}$	−47.77	−5.48
Group 2 ($n=7$)				
Antimicrotubule	Shift-X on O14[c)]	$-0.84^{a)}$	−0.71	3.59
	Shift-Z on O14[c)]	$-0.90^{a)}$	−2.03	−1.46
DNA SSBs	Charge on O26	$-0.81^{a)}$	−47.37	−5.14
	Dipole-Y	$-0.82^{a)}$	−0.74	8.14
	Dipole-T[d)]	$-0.77^{a)}$	−1.05	12.47
Group 3 ($n=5$)				
Antimicrotubule	Shift-X on O14[c)]	−0.90	−0.68	3.39
	Shift-Z on O14[c)]	−0.90	−2.46	−2.38
	Dipole-X	0.81	0.81	0.96
DNA SSBs	Charge on O26	−0.91	−57.43	−7.29
	Dipole-Y	−0.86	−0.87	8.88
	Dipole-T[d)]	$-0.94^{a)}$	−1.45	15.62

n=sample number. R values were examined by means of the t-test; parameters denoted by *a*) were correlated with 95% confidence level. *b*) 99% confidence. *c*) Oxygen bound to C14 or C16. *d*) Dipole-T is total value of dipole moment.

moment and the antimicrotubule activity are observed; this component is affected by the C–D ring junction mode and the configuration of O14 hydroxyl group. The correlation between the dipole Y-component and the DNA SSB activity is also observed in the groups (2) and (3), and this is dependent upon the orientation of the methoxy group attached to the *para* position of E-ring. The total value of the dipole moment also correlates negatively with the DNA SSB activity.

Judging from the results in Table IV and the comparison with the chemical structures in Fig. 1, the antimicrotubule activity is strongly affected by the steric parameters reflecting the spatial positions of each atom, especially of the polar oxygen atom, and the DNA SSB activity by the electrostatic ones resulting the atomic charges and dipole moments. Therefore it appears that the spatial distribution of each atom is important for the binding with tubulin,[18] which relates to the former activity, and the electrostatic parameters, such as the distributions of atomic charges and the directions of dipole moments, are importantly related to the interaction with type II DNA topoisomerase,[5] which relates to the latter one. The present study on the structure–activity relationships has revealed a clear difference of the structural parameters required for the antimicrotubule and DNA SSB activities.

Experimental

Crystallization and Data Collection of 1——Deoxypodophyllotoxin (**1**) was isolated from the roots of *Anthriscus sylvestris* HOFFM. (Umbelliferae).[19] Platelet crystals were grown from 50% ethanol aqueous solution by slow evaporation at room temperature. The density of the crystals was measured by the flotation method in KI aqueous solution. A single crystal was mounted on a Rigaku automated four-circle diffractometer. Using graphite-

TABLE V. The Final Atomic Parameters with Their Estimated Standard Deviations in Parentheses

Atom[a)]	x	y	z	B_{eq}
O1A	0.3312 (5)	0.7900 (3)	0.7439 (2)	8.1 (3)
C2A	0.2553 (7)	0.8232 (5)	0.7807 (2)	7.7 (4)
O3A	0.3272 (4)	0.8962 (4)	0.8049 (2)	8.2 (3)
C4A	0.4468 (5)	0.9089 (4)	0.7830 (2)	4.9 (2)
C5A	0.5480 (5)	0.9716 (4)	0.7927 (2)	4.6 (2)
C6A	0.6616 (5)	0.9681 (3)	0.7662 (1)	3.8 (2)
C7A	0.7723 (5)	1.0427 (3)	0.7778 (1)	3.8 (2)
C8A	0.8682 (6)	1.0453 (4)	0.7381 (2)	4.4 (2)
C9A	0.9999 (7)	1.0997 (4)	0.7416 (2)	5.0 (3)
O10A	1.0275 (5)	1.1774 (3)	0.7616 (1)	6.9 (2)
O11A	1.0897 (4)	1.0494 (3)	0.7164 (1)	6.6 (2)
C12A	1.0306 (6)	0.9607 (5)	0.6943 (2)	6.1 (3)
C13A	0.9083 (6)	0.9365 (4)	0.7222 (2)	4.6 (2)
C14A	0.7899 (6)	0.8885 (4)	0.7003 (2)	4.9 (2)
C15A	0.6680 (5)	0.9001 (3)	0.7309 (2)	4.3 (2)
C16A	0.5558 (6)	0.8356 (4)	0.7201 (2)	5.3 (3)
C17A	0.4515 (6)	0.8433 (4)	0.7468 (2)	5.3 (3)
C18A	0.8382 (5)	1.0207 (3)	0.8225 (1)	3.6 (2)
C19A	0.8682 (5)	0.9183 (3)	0.8352 (1)	3.6 (2)
C20A	0.9318 (5)	0.9020 (3)	0.8763 (2)	3.8 (2)
C21A	0.9623 (4)	0.9841 (4)	0.9043 (1)	3.7 (2)
C22A	0.9266 (5)	1.0820 (3)	0.8920 (2)	3.8 (2)
C23A	0.8659 (5)	1.1011 (3)	0.8511 (2)	4.1 (2)
O24A	0.9675 (4)	0.8047 (2)	0.8913 (1)	4.9 (2)
C25A	0.9612 (6)	0.7227 (4)	0.8597 (2)	5.0 (3)
O26A	1.0309 (3)	0.9657 (3)	0.9435 (1)	5.0 (2)
C27A	0.9592 (7)	0.9663 (7)	0.9817 (2)	8.0 (4)
O28A	0.9623 (4)	1.1599 (3)	0.9216 (1)	5.4 (2)
C29A	0.9440 (7)	1.2631 (4)	0.9066 (2)	6.7 (3)
O1B	0.4134 (5)	0.6148 (3)	0.8414 (1)	6.7 (2)
C2B	0.5411 (8)	0.6174 (5)	0.8173 (2)	8.1 (4)
O3B	0.6149 (5)	0.6996 (3)	0.8344 (1)	6.6 (2)
C4B	0.5506 (5)	0.7355 (4)	0.8701 (2)	4.7 (2)
C5B	0.5891 (5)	0.8124 (3)	0.9000 (2)	4.2 (2)
C6B	0.5028 (4)	0.8337 (3)	0.9362 (2)	3.6 (2)
C7B	0.5473 (5)	0.9171 (4)	0.9689 (2)	3.7 (2)
C8B	0.4705 (5)	0.8989 (3)	1.0127 (2)	3.7 (2)
C9B	0.4910 (5)	0.9699 (4)	1.0528 (2)	4.5 (2)
O10B	0.5909 (4)	1.0069 (3)	1.0674 (1)	5.8 (2)
O11B	0.3741 (4)	0.9838 (3)	1.0743 (1)	5.7 (2)
C12B	0.2707 (6)	0.9208 (5)	1.0527 (2)	6.4 (3)
C13B	0.3216 (5)	0.9035 (4)	1.0043 (2)	4.2 (2)
C14B	0.2834 (5)	0.8067 (4)	0.9790 (2)	5.0 (3)
C15B	0.3800 (5)	0.7834 (3)	0.9413 (2)	4.1 (2)
C16B	0.3449 (5)	0.7065 (4)	0.9095 (2)	5.1 (3)
C17B	0.4300 (6)	0.6850 (3)	0.8751 (2)	4.9 (2)
C18B	0.5332 (4)	1.0269 (3)	0.9499 (2)	3.4 (2)
C19B	0.4466 (5)	1.0473 (3)	0.9151 (1)	3.5 (2)
C20B	0.4361 (5)	1.1473 (3)	0.8981 (1)	3.7 (2)
C21B	0.5143 (5)	1.2280 (3)	0.9151 (1)	3.8 (2)
C22B	0.5965 (5)	1.2064 (3)	0.9518 (2)	3.9 (2)
C23B	0.6077 (4)	1.1075 (4)	0.9680 (2)	3.8 (2)
O24B	0.3538 (4)	1.1736 (3)	0.8632 (1)	6.1 (2)
C25B	0.2445 (6)	1.1122 (4)	0.8551 (2)	5.7 (3)
O26B	0.5095 (4)	1.3232 (3)	0.8960 (1)	6.2 (2)
C27B	0.4134 (9)	1.3872 (5)	0.9107 (2)	9.4 (5)
O28B	0.6634 (4)	1.2903 (2)	0.9674 (1)	5.7 (2)
C29B	0.7483 (7)	1.2758 (4)	1.0054 (2)	6.1 (3)

$B_{eq}=4/3(B_{11}a^2+B_{22}b^2+B_{33}c^2)$. *a)* The suffix letters A and B represent forms A and B of **1**, respectively.

monochromated Cu$K\alpha$ radiation ($\lambda = 1.5405$ Å), the unit cell constants were determined by least-squares calculation with 2θ values of 25 high-angle reflections.

Intensity data of 3316 independent reflections [$F_O > 3\sigma(F_O)$] were obtained using the ω–2θ scanning technique ($\sin\theta/\lambda < 0.590$ Å^{-1}). The scan speed was 4°/min; the background was measured for 5 s. The intensities of four standard reflections measured every 100 reflection intervals showed no structural deterioration due to X-ray irradiation during the measurement of all reflections. Corrections were applied for Lorentz and polarization factors, but not for the absorption effects.

Solution of Crystal Structure of 1——The structure of **1** was solved by the direct method. An electron map was computed with the phase set having the highest figure of merit using 450 reflections with the normalized structure factors $|E| > 1.50$, and this map gave the positions for 36 non-hydrogen atoms in an asymmetric unit. Reasonable positions for remaining non-hydrogen atoms were determined by successive Fourier syntheses. The atomic parameters were refined by the block-diagonal least-squares method with anisotropic temperature factors for the non-hydrogen atoms and isotropic ones for the hydrogen atoms. $\sum w(|F_O| - |F_C|)^2$ was minimized where w represents weight for refinement and was used in the last stage as follows; $w = 1.0/[\sigma(F_O)^2 - 0.226|F_O| + 0.119|F_O|^2]$. The discrepancy index $R(=\sum||F_O| - |F_C||/\sum|F_O|)$ was 0.065. The final positional and thermal parameters for all non-hydrogen atoms are given in Table V. All numerical calculations were performed using the UNICS programs.[20] Atomic scattering factors summarized in the International Tables for X-Ray Crystallography[21] were used.

Conformational Analyses of Podophyllotoxin Analogues——The conformations of seven analogues were constructed by the partial structural modification of **1** (form A). For the conformations of picropodophyllin (**8**), it was also taken into account the ^{1}H-NMR data of deoxypicropodophyllin[13] and Karplus formula[22] parameterized by Bothner-By ($J_{vic} = 7.0 - \cos\theta + 5.0\cos 2\theta$) for the estimations of the possible torsion angles (θ) between hydrogen atoms bound to C- and D-rings.

Each analogue built up was then optimized by using molecular mechanics-based Allinger's force field method,[14] which has been formulated in CHEMLAB-II package[23] as a program MMFF parameterized by Hopfinger.[15] **1** was also optimized by the same method to perform regression analysis under the same condition. Solvent effects were not considered in this optimization.

Calculations of Conformational Parameters——Steric property was expressed by the coordinate shift values (X, Y and Z), from the following three planes, respectively; (1) the best plane of six atoms of B-ring, (2) the plane perpendicular to (1) and parallel to the vector from C16 to C5, and (3) the plane perpendicular to (1) and (2) (see Fig. 6). B-ring was used as conformational fitting plane because of its planarity and positional equality for all analogues. Atomic charges and molecular dipole moments were calculated by CNDO/2 (complete neglect of differential overlap/2) method[16] in the CHEMLAB-II package. The dipole moments were calculated as the components along the X, Y and Z directions perpendicular to (1), (2) and (3) planes, respectively.

Analyses of Structure–Activity Relationships——The antimicrotubule and DNA SSB activities were ranked as $\log(1/C)$; C is the concentration of drug necessary to show a given activity. The relationship between the ranked activities and the conformational parameters was examined by linear regression analysis; the correlation coefficient (R) was calculated, its significance was examined by applying the t-test.[17] Of the two conformers observed in the crystal structure of **1**, form A was used for the above-mentioned study. The same study using form B as the starting conformer gave similar results to the case used form A.

All computations were carried out on the DEC microVAX II computer system at the Computing Center, Osaka University of Pharmaceutical Sciences.[24]

References and Notes

1) B. H. Long, S. T. Musial and M. G. Brattain, *Biochemistry*, **23**, 1183 (1984).
2) J. D. Loike and S. B. Horwitz, *Biochemistry*, **15**, 5443 (1976).
3) L. Wilson, J. R. Bamburg, S. B. Mizel, L. M. Grishan and K. M. Creewell, *Fed. Proc. Fedn. Am. Cos. Exp. Biol.*, **33**, 158 (1974).
4) J. D. Loike, C. F. Brewer, H. Strenlicht, W. J. Gensler and S. B. Horwitz, *Cancer Res.*, **38**, 2688 (1978).
5) L. S. Thurston, H. Irie, S. Tani, F. S. Han, Z. C. Liu, Y. C. Cheng and K. H. Lee, *J. Med. Chem.*, **29**, 1547 (1986).
6) B. F. Cain, *J. Chem. Soc.*, **1961**, 2599.
7) M. Kozawa, K. Baba, Y. Matsuyama, T. Kido, M. Sakai, and T. Takemoto, *Chem. Pharm. Bull.*, **30**, 2885 (1982).
8) Y. Inamori, Y. Kato, M. Kubo, K. Baba, Y. Matsuyama, M. Sakai and M. Kozawa, *Chem. Pharm. Bull.*, **31**, 4464 (1983).
9) Y. Inamori, M. Kubo, H. Tsujibo, M. Ogawa, K. Baba, M. Kozawa, and E. Fujita, *Chem. Pharm. Bull.*, **34**, 3928 (1986).
10) T. J. Petcher, H. P. Weber, M. Kuhn and A. von Wartburg, *J. Chem. Soc., Perkin Trans. 2*, **1973**, 288.
11) H. Yamaguchi, M. Arimoto, M. Tanoguchi, T. Ishida and M. Inoue, *Chem. Pharm. Bull.*, **30**, 3212 (1982).

12) H. Yamaguchi, S. Nakajima, M. Arimoto, M. Tanoguchi, T. Ishida and M. Inoue, *Chem. Pharm. Bull.*, **32**, 1754 (1984).
13) Y. Inamori, Y. Kato, M. Kubo, K. Baba, T. Ishida, K. Nomoto and M. Kozawa, *Chem. Pharm. Bull.*, **33**, 704 (1985).
14) E. L. Eliel, N. L. Allinger, S. J. Angyal and G. A. Morrison "Conformational Analysis," Interscience Publishers, New York, 1981.
15) A. J. Hopfinger and R. A. Pearlstein, *J. Comput. Chem.*, **5**, 486 (1984).
16) J. A. Pople and G. A. Segal, *J. Chem. Phys.*, **44**, 3289 (1966).
17) A. Goldstein, "Biostatics, an Introductory Text," Orion Press, Tokyo, 1964.
18) J. K. Batra, L. Jurd and E. Hamel, *Biochem. Pharmacol.*, **35**, 4013 (1986).
19) M. Kozawa, N. Morita and K. Hata, *Yakugaku Zasshi*, **98**, 1486 (1978).
20) The Universal Crystallographic Computing System-Osaka, The Computer Center, Osaka University, Osaka, Japan, 1979.
21) "International Table for X-Ray Crystallography," Vol. 4, ed. by J. A. Ibers and W. C. Hamilton, Kynoch Press, Birmingham, 1974.
22) A. B. Bothner-By, *Advan. Magn. Reson.*, **1**, 195 (1965).
23) The Chemical Modelling Laboratory-II (Revision 9.1) Copyright by Molecular Design Limited (1987); developed under the direction of A. J. Hopfinger.
24) Tables of observed and calculated structure factors, anisotropic thermal parameters of nonhydrogen atoms, atomic coordinates of hydrogen atoms and short contact atomic pairs less than 3.5 Å are available from one of authors (D.Y.) on request.